

## Effective-medium theory for the fracture of fractal porous media

Robert F. Cook

*IBM Thomas J. Watson Research Center, Yorktown Heights, New York 10598*

(Received 30 June 1988)

A general energy-balance theory is developed for the fracture of fractal porous media using an effective-medium approximation to couple the fracture resistance to the (fractal) mass distribution. The decreasing resistance field derived increases the size and rate of size increase of flaws under the influence of localized loading. A general destabilizing field associated with a uniform applied stress is presented and used to examine the strength behavior: Strength is predicted to scale with the dominant flaw size according to  $\sigma_0 \sim c_0^{(D-3-a)/2}$ , where  $D$  is the fractal dimension of the medium ( $< 3$ ), and  $a$  is an exponent characterizing the variation of the destabilizing field with crack length ( $> 1$ ). Hence, for a given distribution of flaw sizes, a porous fractal medium will exhibit lower, more variable strengths than a homogeneous medium.

Fracture of porous media has been primarily examined by computer simulations of systems of  $L \times L$  bonds, diluted by the removal of bonds to some fraction  $p_c < p < 1$ , where  $p_c$  is a characteristic bond fraction at which a property of interest of the system disappears.<sup>1-7</sup> For example, the scaling of the elastic modulus with  $(p - p_c)$  has been examined,<sup>1,2</sup> as has the way a critical failure stress scales with the system size  $L$  for fixed initial  $(p - p_c)$  and/or distribution of bond strengths.<sup>3,4</sup> Similar simulations have examined the behavior of critical voltages for the analogous systems of electrical fuses.<sup>5-7</sup> Some experimental studies have investigated the modulus<sup>8,9</sup> and fracture<sup>10</sup> of randomly holed films. However, only in a very few cases have connections been made with the energy balance framework of fracture mechanics in the consideration of the behavior of the single (dominant) flaw in a body.<sup>3,11,12</sup> This is a significant omission for two reasons. First, most brittle materials fail by the propagation through the body of a single flaw which interacts with elements of the microstructure (e.g., porosity) which remain essentially static.<sup>13</sup> Second, consideration of the energy exchanges provides constraints on the fracture behavior which must be obeyed, independent of the actual mechanisms of bond rupture or the detailed nature of the stress concentration field about a crack tip.

Crack propagation is mediated by the exchange of mechanical energy  $U_M$  (essentially the elastic strain energy stored in the body less the work done by the applied loading), with surface energy  $U_S$ . Hence, consideration of the variation of the total energy  $U_T = U_M + U_S$  for virtual crack advance yields predictions about the fracture behavior.<sup>14</sup> For example, the strength of a body may be determined by calculating the condition for equilibrium at given crack length (i.e., the first derivative of  $U_T$  is zero) and showing that the equilibrium is unstable (i.e., the second derivative is negative). In his classic 1920 paper Griffith used the first of these conditions to predict correctly the strength behavior of glass.<sup>15</sup> The essential physics of the unstable equilibrium is that a crack advance *decreases* the strain energy in a *volume* of material, whereas the surface energy *increases* merely with crack *area*.

Here we present a general theory for the fracture properties of porous media based on the energy balance ideas, and use this theory to examine the stability and instability of single cracks under general loading conditions. Scaling relationships are derived between the strength of the body and the dominant crack length. Our analysis will be an effective-medium formulation, as the work necessary for incremental crack extension will be coupled to the mean density of bonds on the crack front. This is equivalent to "smearing out" the interatomic bonds to a continuum over the prospective crack path (not necessarily planar) and constraining the crack outline to be similar at all stages of propagation.

The model porous system considered is formed by the aggregation of small particles in multiple generations (Fig. 1).<sup>16</sup> This structure is closely allied to those arising in simulations and, as we shall see, provides a great con-

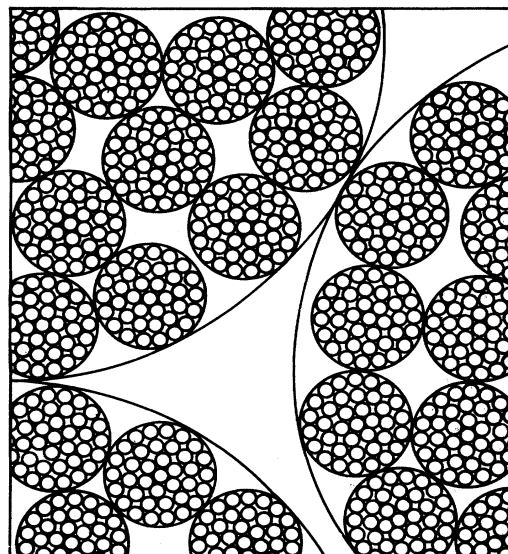


FIG. 1. Schematic of multiple generation aggregates forming a fractal, porous material.

trast with the fracture properties of conventional materials. The mass  $M$  of material as a function of radial coordinate  $r$  is given by  $M(r) = m_0(r/\delta)^D$  where  $m_0$  is the mass of the smallest particle,  $\delta$  is the range of interaction between the particles, and  $D$  is the mass fractal dimension given by  $D = 3 + \ln(P)/\ln(S) \leq 3$  where  $P$  is the packing fraction for a single generation of aggregates and  $S$  is the size ratio between generations of aggregates. The relative density of such a structure is then

$$\rho/\rho_0 = (r/\delta)^{D-3}, \quad (1)$$

where  $\rho_0$  is the effective density of the smallest particle and the upper-bound density of the system. We anticipate that at some large dimension  $\Omega$  the aggregates will begin to pack in a Euclidean way,<sup>16</sup> thereby setting a lower bound on the density. The connectivity threshold  $p_c$  for this system is zero, implying that most choices of  $L/\delta$  and  $D$  will lead to systems outside the "critical region" identified by Sornette,<sup>12</sup> so that effective-medium ideas are applicable.<sup>2</sup> In addition, we assume isotropic force constants between the particles once packed, such that the rigidity and connectivity thresholds are identical.<sup>1,2</sup>

For materials described by Eq. (1) the surface potential energy is

$$U_S = 2\gamma(c/\delta)^{D-3} \alpha_s c^{D_T}, \quad (2)$$

where  $2\gamma$  is the surface energy of the generating particles,  $c$  is the projected crack length,  $\alpha_s c^{D_T}$  is the "extent" of the crack, and  $D_T$  is the topological dimension of the crack [e.g., for a circular crack ( $\alpha, D_T$ ) is ( $\pi, 2$ )]. The scaling of  $U_S$  with the scalar variable  $c$  via the mean density of Eq. (1) is the appropriate effective-medium approximation, rather than the scaling of  $2\gamma$  as used previously.<sup>11</sup> Strictly, Eq. (2) applies only for integer values of  $D_T$  where the areal and lineal relative densities of random slices through the fractal network scale as given by Eq. (1).<sup>17</sup> For noninteger values of  $D_T$ ,  $D$  in Eq. (2) represents the actual variation of bonds encountered by the crack on its (fractal) path, and is related to the mass fractal dimension by a function involving the perturbation of  $D_T$  from an integer. In any event, the limit  $3 - D < D_T$  applies, i.e., the propagating crack cannot remove bonds more rapidly than were omitted in the original aggregation process. The fracture resistance  $R$  (the work per unit area necessary for virtual crack advance) is given by differentiating  $U_S$  with respect to the extent of the crack

$$\begin{aligned} R &= dU_S/d(\alpha_s c^{D_T}) \\ &= 2\gamma(c/\delta)^{D-3} [(D-3+D_T)/D_T] \\ &= \Gamma c^{-g} \end{aligned} \quad (3)$$

shown in Fig. 2. The resistance field decreases with crack length from an upper bound of  $2\gamma$  to a lower bound of  $\Gamma\Omega^{-g}$ , according to the degree of departure of the aggregates from Euclidean packing,  $g = (3-D)$ . The amplitude of the resistance field  $\Gamma$  is proportional to the surface energy of the particles and is held above 0 by the  $(D, D_T)$  constraint above.

The decreasing fracture resistance of such materials is in contrast to the flat  $R$  curves observed in brittle materi-

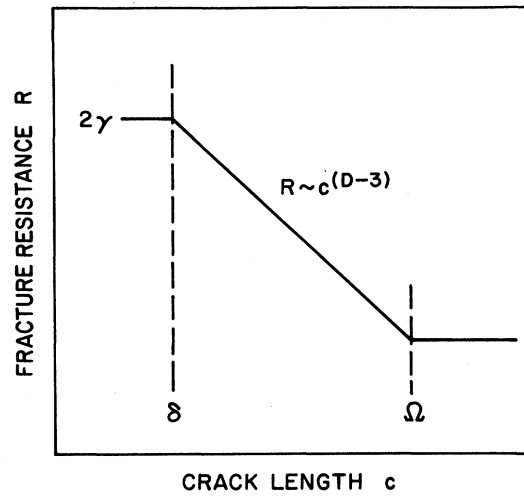


FIG. 2. Variation of the fracture resistance  $R$  with crack length  $c$  for a porous fractal aggregate (logarithmic coordinates).

als such as glass and single crystals where the density of bonds does not vary throughout the material.<sup>13,14</sup> We note in this context that other packing schemes generate different dependencies of density on scale. For example, the packing of uniform disks around a central seed so as to maintain orientational order generates structures which increase toward the Euclidean density as the scale is increased,<sup>18</sup> in contrast to the decreasing density described in Eq. (1). For this latter case, the fracture resistance scales as  $R \sim c^g$ , and the properties of such a resistance field variation have been examined in the context of energy dissipation mechanisms arising during crack propagation.<sup>19</sup>

The parameter characterizing the change in mechanical potential energy  $U_M$  of the system during virtual crack advance is the mechanical energy release rate,  $G = -dU_M/d(\alpha_s c^{D_T})$ . Equilibrium of the fracture system is obtained for  $G = R$  [i.e., for  $d(U_T)/d(\alpha_s c^{D_T}) = 0$ ], and the equilibrium is stable for  $dG/d(\alpha_s c^{D_T}) < dR/d(\alpha_s c^{D_T})$  [i.e., for  $d^2(U_T)/d(\alpha_s c^{D_T})^2 > 0$ ]. We see that the decreasing  $R$  curve for these materials acts to decrease the likelihood of stability. Mechanical energy release rate fields which give rise to stable cracks usually derive from localized loadings and are written generally as<sup>20</sup>

$$G = \Pi c^{-r}, \quad (4)$$

where  $\Pi$  is the amplitude of the field and  $r$  characterizes the geometry of the loading. For  $r > g$  stability is assured, and the stable crack length is obtained by simply imposing the equilibrium condition [equating Eqs. (3) and (4)] to gain

$$c_0 = (\Pi/\Gamma)^{1/(r-g)} \quad (5)$$

shown in Fig. 3. The stable crack length increases with the amplitude of the stabilizing field and decreases with the amplitude of the resistance field. Localized fields are the cause of stable flaws which may only propagate to

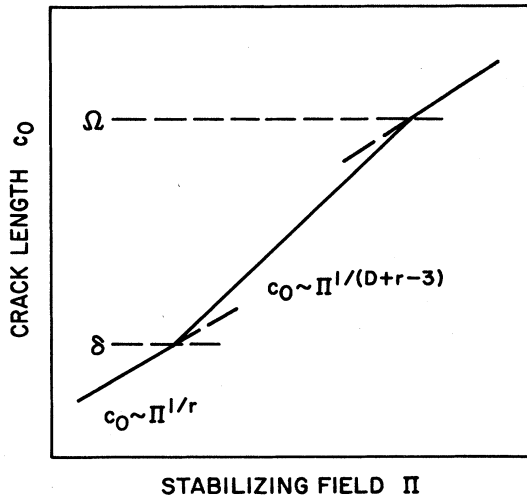


FIG. 3. Variation of crack length  $c_0$  with amplitude of the stabilizing propagation field  $\Pi$  (logarithmic coordinates).

failure under the action of subsequent destabilizing loadings. We see in Fig. 3 that not only are the flaw sizes greater in the fractal region than in the Euclidean region, but that  $c_0$  increases more rapidly with  $\Pi$  in this latter region.

Of perhaps more interest is an unstable equilibrium [ $dG/d(a_s c^{D_T}) > dR/d(a_s c^{D_T})$ ], characterizing the strength of a component. The destabilizing field we consider here is that arising from a uniform stress  $\sigma_a$  imposed over a crack, for which

$$U_M = -\sigma_a^2 a_m c^{D_T + \epsilon} / E,$$

where we scale the extent of the stress concentration field about the crack,  $a_m c^{D_T + \epsilon}$ , with power  $\epsilon$  greater than the extent of the crack. We expect  $\epsilon$  to be close to its upper bound of 1 subject to the constraint of  $D_T + \epsilon \leq 3$ .  $E$  is the Young's modulus. Hence,

$$G = -dU_M/d(a_s c^{D_T}) = \sigma_a^2 c^\epsilon (a_m/a_s) [D_T + \epsilon] / D_T / E. \quad (6)$$

Equation (6) is a lower bound on the  $G(c)$  variation as the crack length dependence of  $E$  has been neglected. In general  $E$  will be a decreasing function of  $c$  (and of  $L$ ),<sup>1,8,9</sup> as fewer bonds per unit volume remain as the crack propagates, and, hence, the general form of  $G$  is

$$G = \Sigma c^a, \quad (7)$$

where  $a \geq 1$ . The amplitude of the destabilizing field  $\Sigma_0$  at unstable equilibrium is given by equating Eqs. (3) and (7) at a crack length of  $c_0$ :

$$\Sigma_0 = \Gamma c_0^{-(a+g)}. \quad (8)$$

Denormalizing Eq. (8) gives the complete scaling law

$$\sigma_0 = (2\gamma E)^{1/2} c_0^{(D-3-a)/2} (a_s/a_m)^{1/2} \times [(D-3+D_T)/(D_T+\epsilon)]^{1/2} / \delta^{(D-3)/2}, \quad (9)$$

which is more general than that given previously,<sup>3,11</sup> and

which is consistent with the limiting solution for infinite homogeneous media ( $a = \epsilon = 1$ ) of<sup>19</sup>

$$\sigma_0 = T / \psi c_0^{1/2}, \quad (10)$$

where  $T = (2\gamma E)^{1/2}$  is the toughness and  $\psi = 2/\pi^{1/2}$  appropriate to a circular crack ( $D, D_T, a_s, a_m$ ) = (3, 2,  $\pi, \frac{8}{3}$ ), or  $\psi = \pi^{1/2}$  appropriate to a linear crack in a body of thickness  $w$  (3, 1,  $2w, \pi w$ ). (This latter configuration is exactly that studied by Griffith.<sup>14</sup>) In both homogeneous and fractal regions the strength scales with the toughness. However, in the fractal region the decrease in strength with crack length is far more rapid, shown in Fig. 4. In this region strength scales as  $\sigma_0 \sim c_0^{(D-3-a)/2}$ , leading to a much broader distribution of strengths for a given distribution of flaw sizes in the fractal region than in the Euclidean regions.

We note that the scaling relationship for strength derived here is very similar to that observed empirically by Beale and Srolovitz<sup>4</sup> in their simulations:  $\sigma_0 \sim c_0^{-1/\mu}$ , for  $1 \leq \mu \leq 2$  in two dimensions. Beale and Srolovitz suggested that the upper bound on  $\mu$  was applicable to isolated defects (corresponding to  $D=3$  and  $a=1$  here, i.e., a homogeneous infinite medium), and the lower bound applicable to adjacent defects (corresponding to the minimum value of  $D=2$  here, for a one-dimensional crack in a maximally porous medium). The scaling of the strength with respect to the size of the body is also similar to that observed empirically. If the pores in these materials are considered to be cracks, as is true in the point connected bonds of the simulations, then the maximum crack size scales as the correlation length  $\xi$ ,<sup>1,3,17</sup>  $c_0 \sim \xi \sim \min(L, \Omega)$ . Hence, for  $L < \Omega$  we have from Eq. (9),  $\sigma_0 \sim L^{(D-4)/2}$ , which compares with  $\sigma_0 \sim L^{-2/\mu m}$  derived by Beale and Srolovitz for the mean strength of a body with flaws distributed with Weibull modulus  $m$ , and which they observed empirically to describe their data for low  $m$ . We note the further identification of  $-1/\mu$  with  $(D-4)/2$  suggested by comparison with the critical defect size. For  $L > \Omega$  the strength of the body is independent of the size of the body

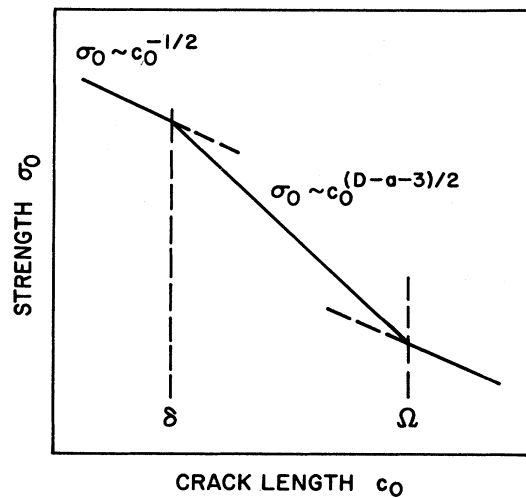


FIG. 4. Variation of strength  $\sigma_0$  with flaw size  $c_0$  (logarithmic coordinates).

and scales with the maximum flaw size as  $\sigma_0 \sim \Omega^{(D-4)/2}$ .

A quantitative estimate of the proportionality constant in the relationship  $c_0 \sim \min(L, \Omega)$  involves consideration of the second moment of the mass distribution, the lacunarity or "gappiness."<sup>17</sup> The relationship between  $P$ ,  $S$ , and  $D$  generates a family of structures with the same value of  $D$  governing the change in the first moment of the mass distribution (the mean bond density change with  $r$ ), but with different second moments (the local bond density in a particular body of size  $L$ ). Calculation of the lacunarity should provide a link between this work and the scaling arguments of Duxbury, Leath, and Beale<sup>5</sup> and may provide an explanation for the intermediate strength distributions found in some simulations.<sup>4,6</sup>

In closing, we note that the general scaling laws for fracture developed here [Eqs. (5) and (8)] will also be applicable to dielectric breakdown where similar propaga-

tion and resistance fields may be defined.<sup>21</sup> Many breakdown and fracture processes in real materials however, occur far from equilibrium, such that perturbations in the loading (mechanical or electrical) occur on time scales commensurate with the rate of bond rupture.<sup>20,22</sup> Hence, the estimates presented here, as well as the results of simulations, made in the "thermodynamic limit,"<sup>5-7</sup> should be seen as the upper bounds on the strength.

The author thanks G. Y. Onoda for the use of Fig. 1, and T. M. Shaw and M. D. Thouless for useful criticism of the manuscript. Figure 1 is reprinted with permission from the American Ceramic Society from "Fractal Dimensions of Model Particle Packings Having Multiple Generations of Agglomerates," by George Y. Onoda and John Toner in *Commun. Am. Ceram. Soc.* **69**, No. 11, C278 (1986), copyright 1986.

<sup>1</sup>S. Feng and P. N. Sen, *Phys. Rev. Lett.* **52**, 216 (1984).

<sup>2</sup>S. Roux and E. Guyon, *J. Phys. (Paris) Lett.* **46**, L999 (1985).

<sup>3</sup>P. Ray and B. K. Chakrabarti, *J. Phys. C* **18**, L185 (1985).

<sup>4</sup>P. D. Beale and D. J. Srolovitz, *Phys. Rev. B* **37**, 5500 (1988);  
D. J. Srolovitz and P. D. Beale, *J. Am. Ceram. Soc.* **71**, 362 (1988).

<sup>5</sup>P. M. Duxbury, P. L. Leath, and P. D. Beale, *Phys. Rev. B* **36**, 367 (1987).

<sup>6</sup>M. D. Stephens and M. Sahimi, *Phys. Rev. B* **36**, 8656 (1987).

<sup>7</sup>B. Kahng, G. G. Batrouni, S. Redner, L. de Arcangelis, and H. J. Herrmann, *Phys. Rev. B* **37**, 7625 (1988).

<sup>8</sup>L. Benguigi, *Phys. Rev. Lett.* **53**, 2028 (1984).

<sup>9</sup>J. Sofo, J. Lorenzana, and E. N. Martinez, *Phys. Rev. B* **36**, 3960 (1987).

<sup>10</sup>K. Sieradzki and R. Li, *Phys. Rev. Lett.* **56**, 2509 (1986).

<sup>11</sup>K. Sieradzki, *J. Phys. C* **18**, L855 (1985).

<sup>12</sup>D. Sornette, *Phys. Rev. B* **36**, 8847 (1987).

<sup>13</sup>R. F. Cook, C. J. Fairbanks, B. R. Lawn, and Y.-W. Mai, *J. Mater. Res.* **2**, 345 (1987).

<sup>14</sup>Y.-W. Mai and B. R. Lawn, *Annu. Rev. Mater. Sci.* **16**, 415 (1986).

<sup>15</sup>A. A. Griffith, *Phil. Trans. R. Soc. London* **221**, 163 (1920).

<sup>16</sup>G. Y. Onoda and J. Toner, *J. Am. Ceram. Soc.* **69**, C278 (1986).

<sup>17</sup>B. B. Mandelbrodt, *The Fractal Geometry of Nature* (Freeman, New York, 1983).

<sup>18</sup>G. Y. Onoda and J. Toner, *Phys. Rev. B* **35**, 3437 (1987).

<sup>19</sup>R. F. Cook and D. R. Clarke, *Acta Metall.* **36**, 555 (1988).

<sup>20</sup>R. F. Cook (unpublished).

<sup>21</sup>E. J. Garboczi, *Phys. Rev. B* **38**, 9005 (1988).

<sup>22</sup>R. F. Cook, *J. Mater. Res.* **1**, 852 (1986).